3
Competitive binding of OP with BSA

3.1 INTRODUCTION

In Vitro analysis of the interaction of organophosphate pesticides (OP) with bovine serum albumin (BSA) is crucial to understand their potential effects at the molecular level. As discussed in section 1.4 (Chapter 1), it is evident that qualitative as well as quantitative analysis of such interaction has drawn considerable attention over the years [Dahiya et al, 2019; Suganthi and Elango, 2017a; Weber et al, 2017; Cartier et al, 2016; Curl et al, 2015; Goncharov et al, 2015; Magnarelli and Fonovich, 2013; Han et al, 2012; Smith et al, 2010; Ageda et al, 2006; Silva et al, 2004; Gollapudi et al, 1995; Mourik and Jong, 1978; Haque et al, 1973;]. In this Chapter, the major focus is to employ magnetization transfer-based solution-state NMR methods, namely ^{1}H Saturation Transfer Difference (STD) NMR experiments, to quantitate the interaction of a set of OP *viz.* chlorpyrifos (CPF), diazinon (DZN) and parathion (PA) with BSA. CPF, DZN, and PA, classified as class II OP can cause acute poisoning by indirect exposure to non-targeted animals, as discussed previously in Chapter 1 [Davies and Holub, 1980; Jafari et al, 2018; John and Shaike, 2015a; Osman, 2011; Narang et al, 2015; Wang et al., 2011]. Figure 1.11-1.13 (Chapter 1) represent the molecular structures of the chosen set of OP. Furthermore, molecular docking and Isothermal Titration Calorimetry (ITC) have also been employed for the complete unraveling of the binding interaction of the chosen set of OP with BSA in solution [Dahiya et al.,2020]. Figure 3.1 gives a graphical illustration of the experimental methods used to investigate the said OP-BSA interaction. It is well established in the literature that the interaction of OP with serum protein strongly influences their ADMET (absorption, distribution, metabolism, excretion, and toxicity) [Suganthi & Elango, 2017a].

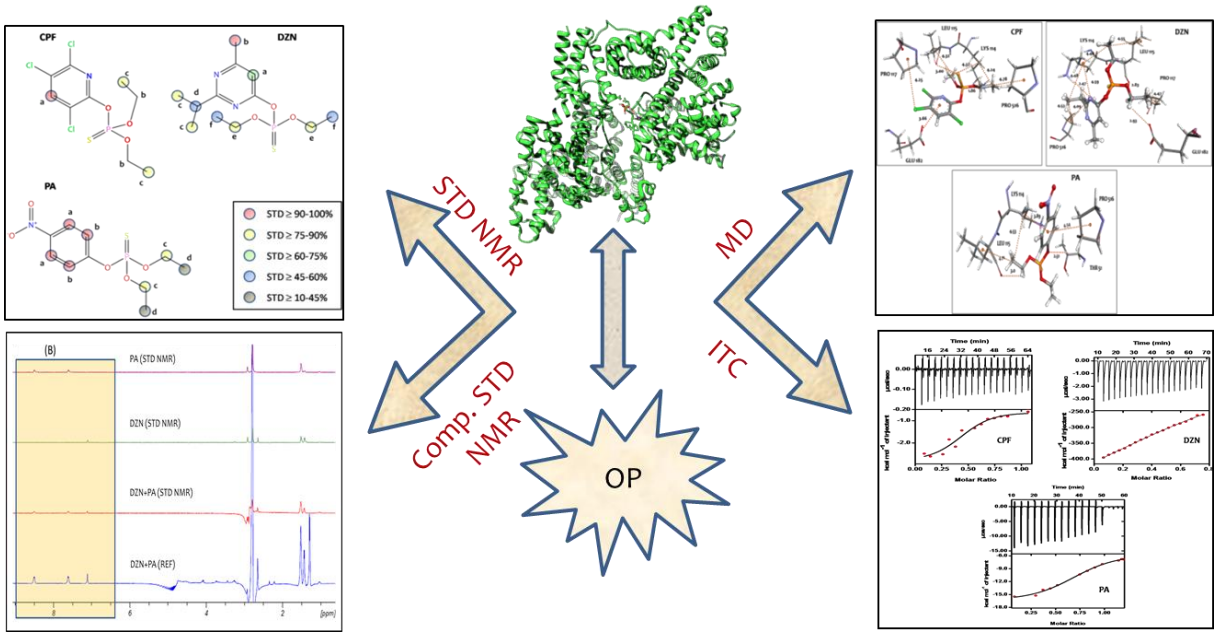

Figure 3.1 : The schematic representation of OP-BSA interaction.

The present investigation of the binding characteristics of OP-BSA, therefore, helps analyze the physiological effect at the molecular level allowing the understanding of relevant health risks of these OP. The key goals of this study are as follows:

(i) Evaluation of the binding affinity of OP-BSA complex by STD NMR: (a) Group-epitope mapping (GEM) for OP-BSA interaction [Meyer et al, 2004; Wagstaff et al, 2013]; (b) extraction of dissociation constant (K_D) [Krishnan, 2005; Meyer and Peters, 2003b; Monaco et al, 2017a; Unione et al, 2014]; (c) determination of protein binding site using protein site-marker STD experiment [Yang et al, 2017]; (d) detection of high-affinity OP using competition STD experiments for a mixture of OP [Wang et al, 2004],

(ii) Determination of binding forces from molecular docking [Suganthi & Elango, 2017a]

(iii) ITC for thermodynamic parameters and binding stoichiometry determination [Yang et al, 2017].

This set of analysis could be helpful in describing the diversity in the distribution and fate of OP within living systems. Further, it would be beneficial in understanding the interfering mechanism of OP poisoning resulting in the detrimental effect of OP exposure on human and animal health. This study may further pave the approach for designing biomonitoring methods of OP.

3.2 SAMPLE PREPARATION

For STD NMR measurements, the BSA stock was prepared in deuterated phosphate buffer (PB) (0.05 M) of pH 7.4. The stock solutions of CPF, DZN, PA, warfarin (WAR) and ibuprofen (IBU) were prepared in DMSO-d_6 due to low solubility of OP in water [Bonechi et al, 2006; Ma et al, 2016b; Martini et al, 2010; Rossi et al, 2001]. The solvent combination of 3:2 D_2O: DMSO was used for further dilutions of NMR samples. For the STD build-up curve, the ligand: protein ratio was fixed at 40:1 (400 µM:10 µM). The dissociation constant measurement (K_D) was performed with ligand concentration varying from 0.4-1.2 mM. The site-marker competitive STD experiments were performed using 400 µM OP and 10 µM BSA with 400 µM WAR/ IBU concentration.

Further, for ITC measurements, the BSA solution was initially prepared in PB with 5% DMSO, and the respective ligand dilutions were prepared in the same buffer with pH 7.4. The final concentrations of the protein samples were analyzed using Nanodrop using the molar extinction coefficient (ε) (43824 M^{-1} cm^{-1}) of BSA at 280 nm [Anand et al, 2018].

3.3 EXPERIMENTAL DETAILS

3.3.1 STD NMR Experiments

All NMR measurements were performed at 298 K using a Bruker Ascend 500 MHz wide-bore NMR spectrometer equipped with a BBFO probe head. Chemical shifts were referenced to the residual water signal at 4.69 ppm. To acquire and process NMR data, Bruker software TopSpin 3.2 was used. STD experiments were performed by using a train of 50 ms Gaussian-shaped pulses separated by a 1 ms delay to selectively saturate protein signals at 298 K. 30 ms spin-lock pulse was used to suppress protein resonances. The STD pulse sequence is preceded by water suppression using excitation sculpting pulses, as reported by Mayer et al [Mayer and Meyer, 2001]. The on-resonance saturation was accomplished using the Gaussian pulse train at -0.6 ppm while the same train applied at 40 ppm allowed the recording of the STD control (off-resonance) experiment. The STD build-up intensities plotted against a range of saturation times 0.5, 1, 2, 3, 4, and 5 s were fitted to a mono-exponential curve [Meyer et al, 2004]. The STD spectra were integrated with reference to the STD_{off} spectrum, and the proton with the highest STD value was

assigned as receiver of 100% saturation. For all other protons, the degree of saturation was calculated with respect to the above-mentioned proton receiving 100% saturation. K_D values of OP-BSA complexes were extracted by employing nonlinear least-square fit of the STD amplification factors plotted as a function of the varying ligand concentrations from 0.4-1.2 mM [Krishnan, 2005; Mayer and Meyer, 2001; Mayer and Meyer, 1999; Meyer and Peters, 2003a]. The STD intensity (I_{STD}) is calculated by Eq.(2.2) (Chapter 2). The STD build-up curve and dissociation constant (K_D) of OP-BSA interaction were calculated by using Eqs.(2.4) and (2.5), as mentioned in Chapter 2. Table 3.1 summarizes all the experimental parameters used for STD NMR experiment.

Table 3.1 : Experimental parameters used to obtain the STD NMR spectrum.

Experimental parameters	**Values**
Pulse program	STDDIFFESGP.3
Number of scans	2048
Saturation time	2 s (K_D determination)
Shaped pulse for saturation	50 ms Gaussian pulses
On-resonance frequency	-0.6 ppm
Off-resonance frequency	40 ppm
Spin lock time	30 ms
Shaped pulse for solvent presaturation	Squa100.1000

3.3.2. Molecular Docking Details

To identify the potential interacting residues between OP-BSA complex, Discovery studio 4.0 was used. The structures for the ligand molecules were obtained from PubChem with PDB IDs CID:2730 for CPF, CID:3017 for DZN, and CID:99 for PM. The ligand molecules were initially prepared for interaction studies using 'prepare ligand wizard' of the Discovery studio 4.0 (DS4). The ligands were at first pre-processed using a pH-based ionization method. The 3D X-ray crystal structure of BSA (PDB ID: 4F5S), used in the docking study, was obtained from Protein Data Bank (PDB). Prior to docking, the protein molecule was prepared through 'prepare protein wizard' of DS4. The pre-processed structures were obtained by removing water and hetero atoms leaving a nascent BSA molecule. The pre-processing and protonation were carried out using CHARMm force fields with a predefined ionic strength at pH 7.4. The CHARMM force fields were applied to these molecules [Anand et al, 2017; Brooks et al, 2009]. The ligands were then docked into a specific receptor site of BSA molecule, as already reported in PDB. The docking steps were carried out for 10 different conformations with 10 different orientations by employing a refined CDocker protocol [Robertson et al , 2003]. The simulations were executed in a Dell precision T5610 workstation [Anand et al, 2017].

3.3.3 Isothermal Titration Calorimetry Analysis

To gain more insights into the thermodynamic parameters between OP-BSA system, Isothermal Titration Calorimetry (ITC) using MicroCaliTC nano200) at 298 K was employed. Prior to injection into the reaction cell, all the sample solutions were carefully degassed and equilibrated at 4 °C. In brief, ~200 µM of ligand was injected to the protein samples of 20 µM after an initial

delay of 60 seconds with a flow rate of 2 µM per injection at a time spacing of 180 seconds with a filter period of 5 seconds each. All these experiments were performed in a high feedback gain mode with a DP (differential power) of 10 µcal/sec at 250 rpm. The obtained data were analyzed and fitted using the inbuilt Origin software to extract the protein-ligand interaction parameters.

3.4 RESULTS AND DISCUSSION

3.4.1 Identification of OP-BSA Binding by STD NMR

One dimensional (1D) ^{1}H NMR spectra of CPF, DZN, and PA in the absence and presence of BSA are recorded and compared in terms of changes in the ^{1}H chemical shift positions and line width for preliminary confirmation of the binding event, as shown in Figure 3.2.

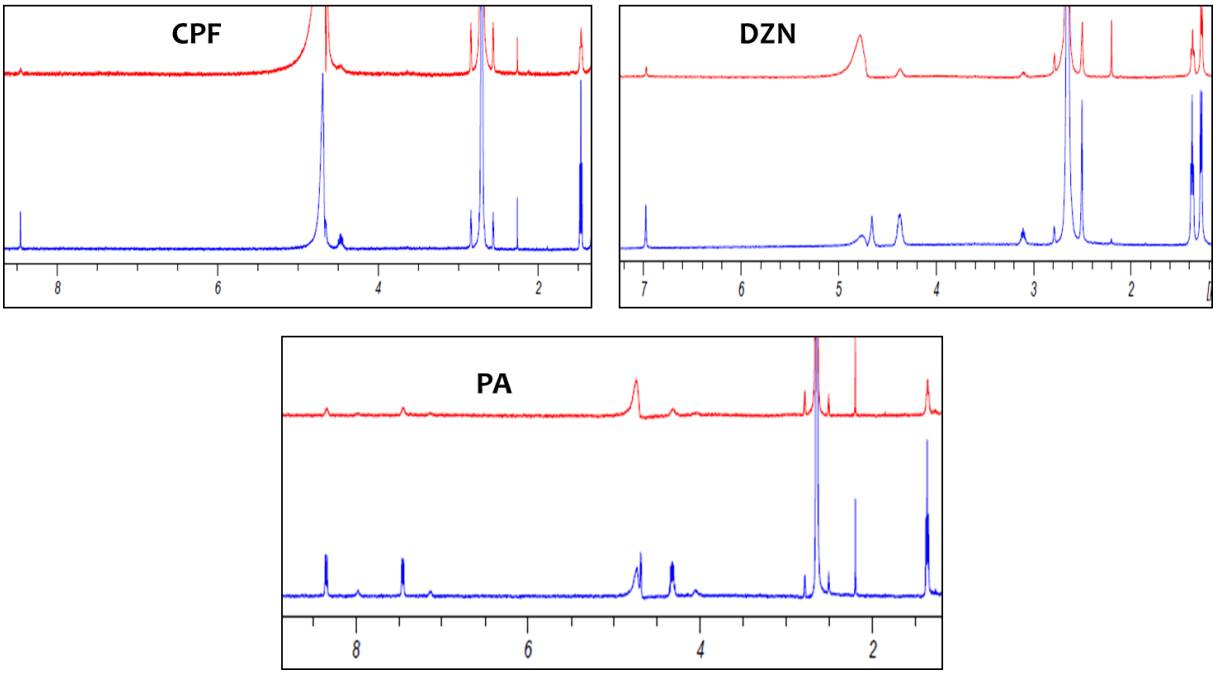

Figure 3.2 : ^{1}H NMR spectra of CPF, DZN, and PA in absence and presence of BSA recorded at room temperature and pH 7.4.

Following these spectra, the 1D ^{1}H STD NMR experiments are performed with a ligand: protein concentration of 40:1 ratio for all the three OP-BSA systems. To quantify the OP-BSA interaction, the K_D is calculated for each OP-BSA complex using STD NMR with varying ligand concentrations, while protein concentration is kept constant. Figure 3.3 represents the STD spectrum of the three OP *viz*. CPF, DZN, and PA in the presence of BSA.

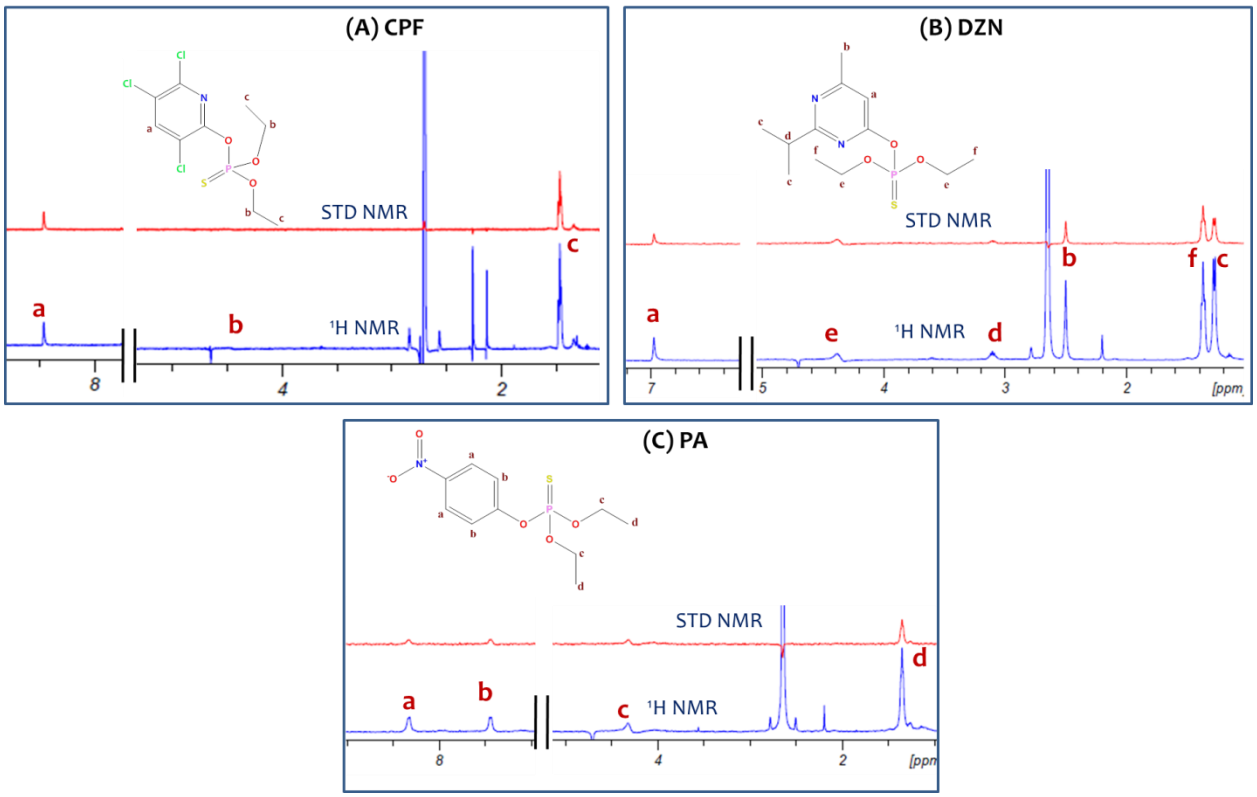

Figure 3.3 : (A) ^{1}H NMR spectrum and ^{1}H STD NMR spectrum of CPF in the presence of BSA in 40:1 ratio; (B) ^{1}H NMR spectrum and ^{1}H STD NMR spectrum of DZN in the presence of BSA in 40:1 ratio; (C) ^{1}H NMR spectrum and ^{1}H STD NMR spectrum of PA in the presence of BSA in 40:1 ratio; Spectra are taken at 298 K on a 500 MHz spectrometer at 298 K. NS=2048, TD = 32 K.

Further, the Group Epitope Mapping (GEM) is identified by calculating the relative STD (%) (R_{STD}). As discussed in section 2.3.3, GEM reflects the spatial proximity of ligand protons with the protein protons by using the relative saturation transfer. The R_{STD} represents the amount of saturation received by the ligand proton from protein proton via intermolecular dipolar interaction [Angulo et al, 2010; Mayer and Meyer, 1999]. For quantitation of R_{STD} for each ligand proton, the STD signal with the highest integral value is set at 100% and represented as R_{STD}^{100}. For all other protons, the STD signals are integrated with reference to R_{STD}^{100}. For CPF, the most intense STD signal is observed for H_a proton that is set as R_{STD}^{100}. This suggests that the ring proton is in close proximity to the surface of BSA. Consequently, the intensity of H_c proton is calculated to be 70.6% with respect to the H_a presented in Figure 3.4. However, the spectral integration of proton H_b is difficult due to overlap with water protons.

A similar exercise is followed for DZN and PA, and the various R_{STD} values obtained for all the three ligands are tabulated in Table 3.2. In the case of DZN, the H_b proton receives the highest saturation. The relative STD % for protons H_a, H_c, and H_d are very similar whereas, the H_f and H_e exhibits the lowest saturation transfer. On the other hand, for PA, the highest saturation transfer is measured for H_a and H_b while the least saturation is received by H_c.

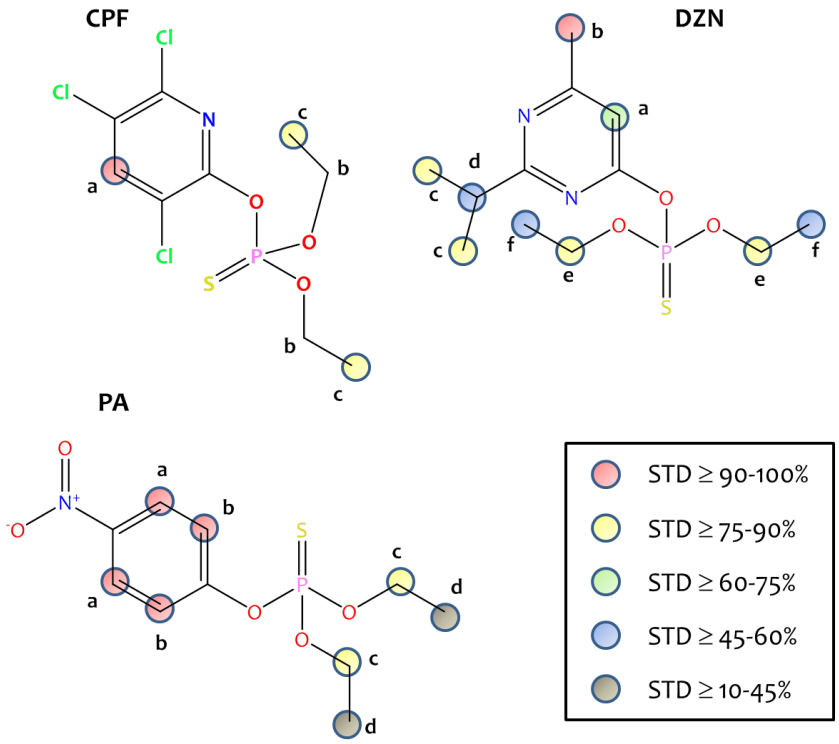

Figure 3.4 : The pictorial representation of GEM for CPF, DZN, and PA. The relative degree of saturation of hydrogen is mapped for CPF, DZN, and PA. The ratio of intensity is normalized using the highest STD H_a for CPF and PA and H_b for DZN (100%) as a reference. (Color code represents the relative STD %).

Table 3.2 : R_{STD} (%) value for CPF-BSA, DZN-BSA and PA-BSA complex. The symbol * denotes proton could not identified and # represents proton does not exist.

OP	Chlorpyrifos R_{STD} (%)	Diazinon R_{STD} (%)	Parathion R_{STD} (%)
H_a	100	70.1	100
H_b	*	100	98.9 %
H_c	70.6%	78.2%	11.6%
H_d	#	78.1	84.1 %
H_e	#	49.2 %	#
H_f	#	51.3%	#

The experimental observation of R_{STD} values made in case of these OP can be summarized as follows: i) in all the cases, the most intense STD signals are observed for the ring protons of the aforementioned OP (CPF, DZN, and PA), suggesting that the ring moiety is in close proximity with the BSA binding sites, (Figure 3.4) [Gairí et al, 2016; Krishnan, 2005; Mayer and Meyer, 2001; Nobrega and Cabrita, 2011; Reddy et al, 2015]; ii) due to steric hindrance, the methylene protons present in these OP most probably remain significantly away from the protein protons and therefore receive less saturation compared to the ring protons; iii) the R_{STD} values calculated for each ligand indicated that the test OP have similar binding modes towards BSA; to be precise, the binding occurs through the ring moiety of the test OP.

To determine the STD amplification factor, the STD build-up experiments are performed with varying protein saturation time ranging from 0.5-5 s for the test OP at a ligand to protein ratio 40: 1 as represented by Figure 3.5. The STD_{max} (maximal STD intensity), and k_{sat} (saturation rate constant) are obtained for all the three OP by using Eq.(2.4) as the fitting Equation. At maximum saturation time, the build-up curve becomes flattened, because of relaxation rate of saturated ligand in the free state. Table 3.3 documents experimentally derived STD_{max} and k_{sat} values for all the three OP.

Table 3.3 : STD_{max} and k_{sat} values for CPF, DZN, and PA.

Proton	**STD_{max}**	**k_{sat} (s^{-1})**	**STD_{max}**	**k_{sat} (s^{-1})**	**STD_{max}**	**k_{sat} (s^{-1})**
	Chlorpyrifos R^2=0.961		Diazinon R^2=0.98		Parathion R^2=0.98	
H_a	21.35±0.48	1.34±0.12	21.03±1.65	0.38±0.06	12.88±1.39	0.76±0.05
H_b	Could not identified		24.27±1.44	0.64±0.01	12.67±0.638	0.72±0.09
H_c	18.46±0.54	1.22±0.14	18.06±1.02	0.61±0.09	1.48±0.12	1.85±0.74
H_d	Protons does not exist		11.67±1.16	0.49±0.01	11.68±0.69	0.54±0.08
H_e			19.26±2.3	0.42±0.09	Protons does not exist	
H_f			8.96±0.61	0.76±0.06		
H_d			11.68±0.69	0.54±0.08		

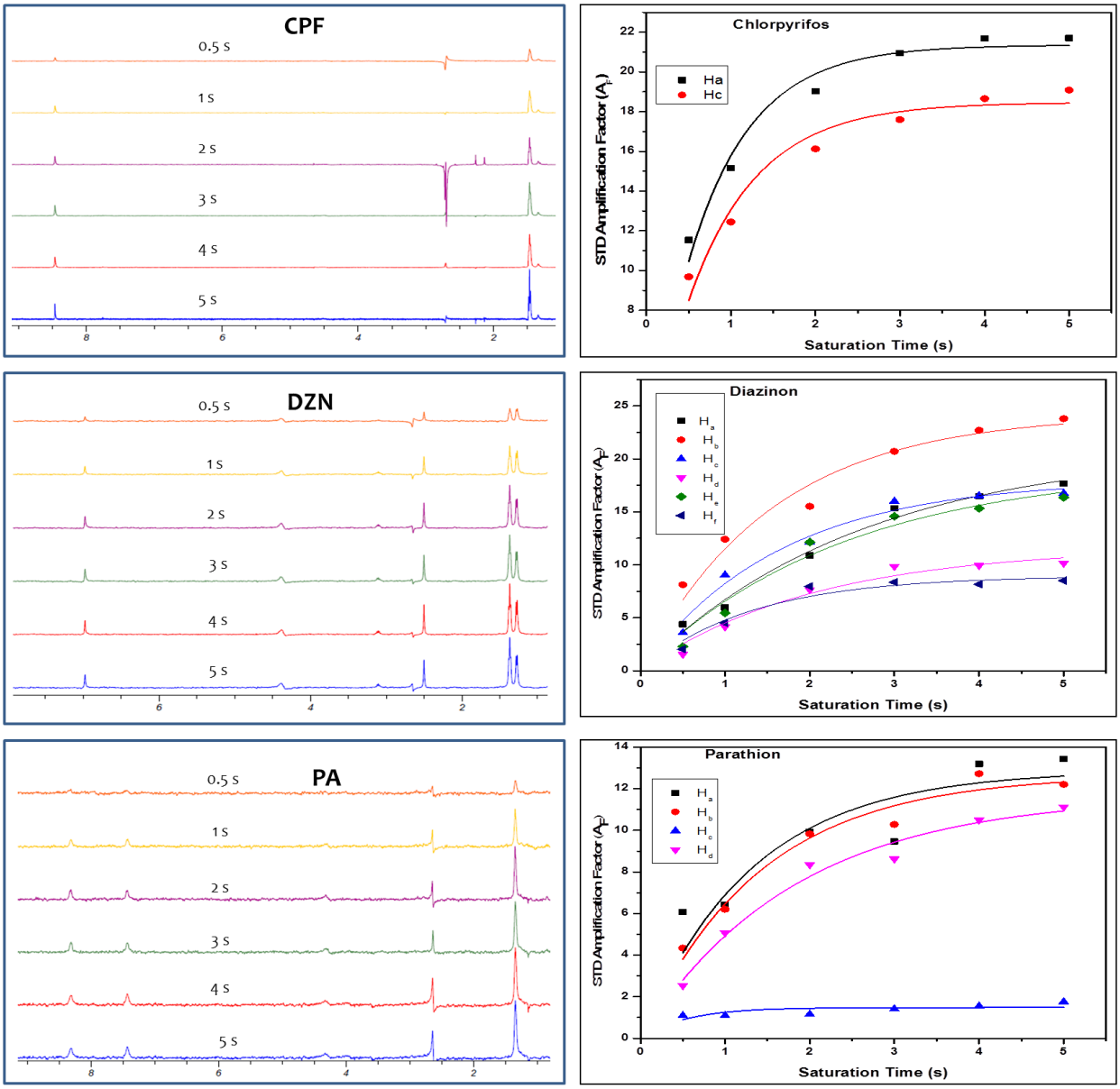

Figure 3.5 : STD amplification factor of CPF, DZN, and PA as a function of saturation time.

While varying the saturation time from 0.5-5 s during the acquisition of STD build-up curves, it is found that 2 s saturation time is the most efficient in terms of saturating the protein signals. Therefore, 2 s saturation time is used for further titration experiments with varying ligand concentrations.

3.4.2 K_D Determination

STD amplification with varying ligand concentrations for test OP is used to determine the binding strength. The ligand titration experiment (0.4 to 1.2 mM) is used to calculate the OP-BSA dissociation constants (K_D) with constant saturation time (2 s). The K_D values are calculated by using Eq.(2.5) (Chapter 2), by plotting the A_F (STD amplification factor) against ligand concentration (Figure 3.6).

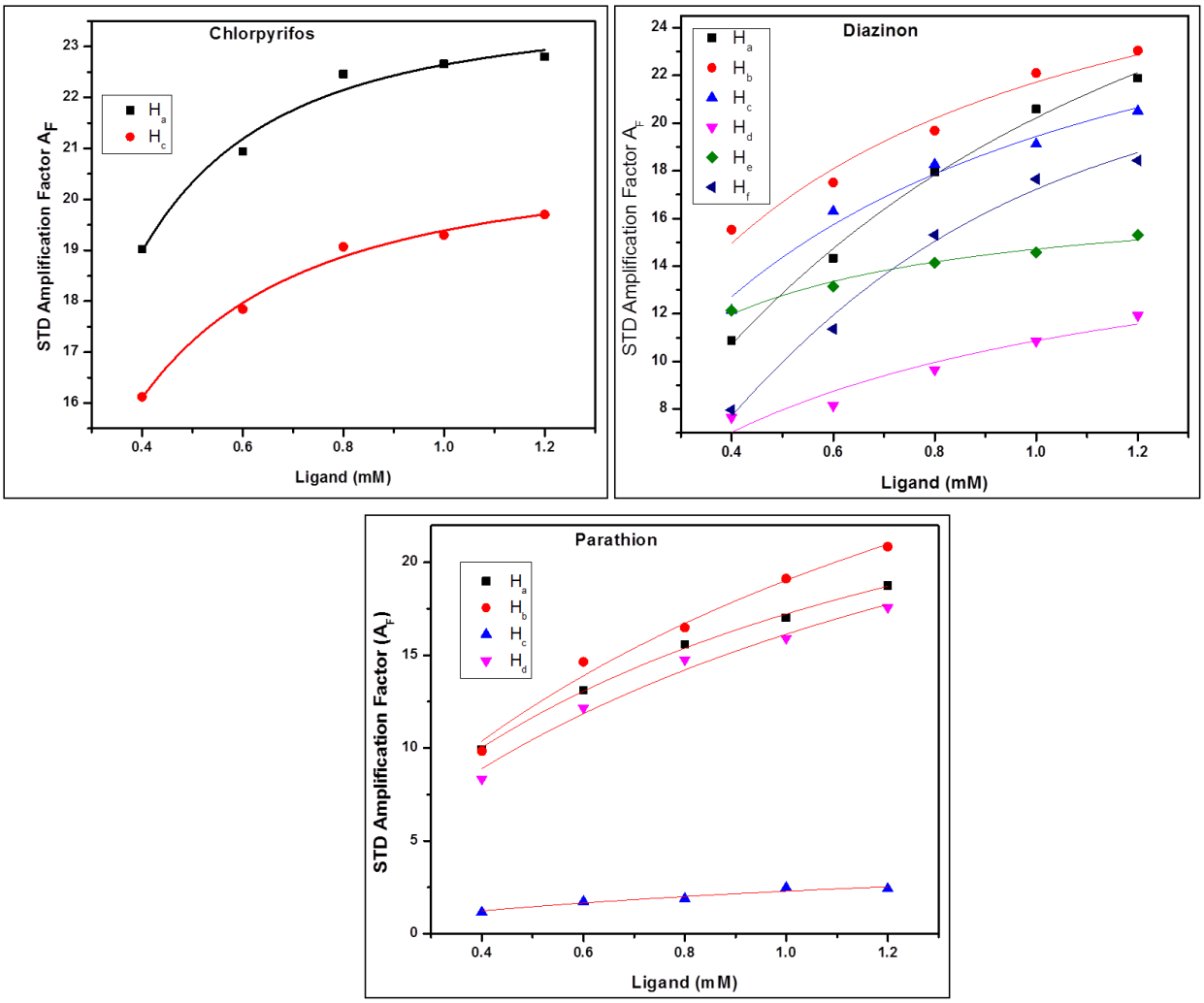

Figure 3.6 : STD amplification factor (A_F) curves with varying ligand concentration (CPF, DZN, and PA) from 400 µM -1.2 mM, keeping BSA concentration constant (10 µM). 2 s saturation time is used at 298 K temperature on 500 MHz NMR.

The experimentally determined K_D values for each proton in the case of all the three OP are given in Table 3.4. It is to be noted here that some of the K_D values reported in the Table 3.4 exhibit large uncertainties due to error in spectral integration caused either by signal overlap with water proton (H_b proton for CPF) or due to phase distortion of spectral lines (H_d and H_e proton for DZN, and H_e proton for PA) or due to overlap with carbon satellite of DMSO (H_b proton for DZN). These K_D values are then neglected for subsequent determination of the average K_D.

Table 3.4 : K_D value for CPF-BSA, DZN-BSA, and PA-BSA.

CPF K_D **(M)** $\times 10^{-4}$ R^2 =0.965		**DZN** K_D **(M)** $\times 10^{-3}$ R^2 =0.990						**PA** K_D **(M)** $\times 10^{-3}$ R^2 =0.997			
H_a	H_c	H_a	H_b	H_c	H_d	H_e	H_f	H_a	H_b	H_c	H_d
1.86 ±0.39	1.78 ±0.24	1.29 ±0.18	0.43 ±0.07	0.54 ±0.09	0.57 ±0.17	0.18 ±0.02	2.08 ±0.82	0.91 ±0.06	1.25 ±0.25	1.34 ±0.64	1.18 ±0.25

The average K_D for OP-BSA is given in Table 3.5. Direct comparison of experimentally determined K_D values for all the three OP clearly indicate that CPF-BSA exhibits *ca*., 10 times stronger association as compared to that of DZN-BSA and PA-BSA. As already mentioned in the previous section that the binding mode is similar for all the three OP, that is, the binding is happening through the aromatic ring. Hence the difference in association ability can be only due to the chemical substituents present on each ring. CPF possesses three chlorine atoms, while DZN contains only aliphatic groups as substituents. On the other hand, PA has nitro group as the substituent. Since the association behavior of DZN and PA are almost equal to each other, this means the electron-withdrawing effect of nitro and electron-donating effect of aliphatic groups do not influence the association differently. However, in the case of CPF, the chlorine groups can exert halogen interaction with protein. CPF contains three chlorine (–Cl) atoms in the ring resulting in halogen bonding with the protein binding sites. [Lin and Mackerell, 2017; Shinada et al, 2019; Wilcken et al, 2013]. The relevance of halogen bonding in biological systems is well known in the literature that documents halogen-bonding between a halogenated ligand and protein backbone and side-chain having Lewis base like the character [67]. The ligand-protein interaction is generally described by considering one or two interactions for each atom. Since, the atoms are generally in contact with numerous other atoms, and therefore, numerous interactions can co-occur at the same halogen atom. Due to its anisotropic electron distribution, halogens can act as both a halogen bond donor and a hydrogen bond acceptor. The various possible hypotheses related to halogen bonding relevant for Ligand-Protein interaction can be discussed as follows:

1. σ-hole: Halogen contains an anisotropic charge distribution with an equatorial negative charge on one region and a positive electrostatic potential on the outer region (σ-hole), leading to halogen bonding. In literature it is well reported that ligands with halogen atoms exhibit stronger affinity towards proteins via such halogen bonding [Lin and Mackerell, 2017; Shinada et al, 2019; Wilcken et al, 2013]. The results confirm that the structure plays an essential role in binding with protein.
2. π-hole: The electron-withdrawing groups have a major effect on the electron delocalization for aromatic groups where lone pairs extend in the ring's plane; Therefore, fluorine and chlorine atoms attract electrons toward their position on the ring, result in two electron-depleted regions on both sides of the aromatic ring plane called π-hole.
3. Hydrophobic interaction: The polar atoms located in the neutral region of halogen can play an important role in the binding mechanism by contributing to hydrophobic components. It is well reported in the literature that the methyl group is the most frequently occurring hydrophobic moiety in contact with a halogen atom (more than 50% for fluorine and chlorine elements), followed by −CH2 moiety with around than 35%. The presence of hydrophobic interactions in ligand-protein interaction will increase affinity through entropy gain.

Table 3.5 : Average Dissociation Constant (K_D) Values for CPF-BSA, DZN-BSA, and PA-BSA system.

CPF K_D **(M)** $\times 10^{-4}$ R^2 **=0.965**	**DZN** K_D **(M)** $\times 10^{-3}$ R^2 **=0.990**	**PA** K_D **(M)** $\times 10^{-3}$ R^2 **=0.997**
1.82±0.31	1.30±0.36	1.11±0.18

3.4.3 Binding Site determination

For binding site determination, the protein site-marker experiment with a known competitive molecule (spy molecule) for a particular site is used with the test molecule. BSA contains three homologous domains (I–III) with two subdomains named A and B in each domain [X. M. He & Carter, 1992]. Competition STD NMR experiments are performed using warfarin (chemoprophylaxis agent) and ibuprofen (nonsteroidal anti-inflammatory drug), well known BSA site markers for the site I (subdomains IIA) and site II (subdomains IIIA), respectively [Dahiya and Pal, 2018; Ma and Wang, 2016; Rahman et al, 2005; Rezner and Sułkowski, 2005]. In general, the competitive molecule in the solution with unknown ligand concentration can either diminish or intensify the ligand signal intensity in the STD spectrum when the competitive molecule is a better binder to the same site [Monaco et al, 2017b; Tanoli et al, 2015; Wang et al, 2004; Yang et al, 2017]. Figure 3.7 shows the ^{1}H NMR and ^{1}H STD-NMR spectra for the OP-BSA system after adding BSA site-markers. In the case of CPF–BSA (Figure 3.7 (A)), both WAR and IBU affect the STD intensity, which illustrates that both warfarin and ibuprofen competed with CPF to interact with BSA.

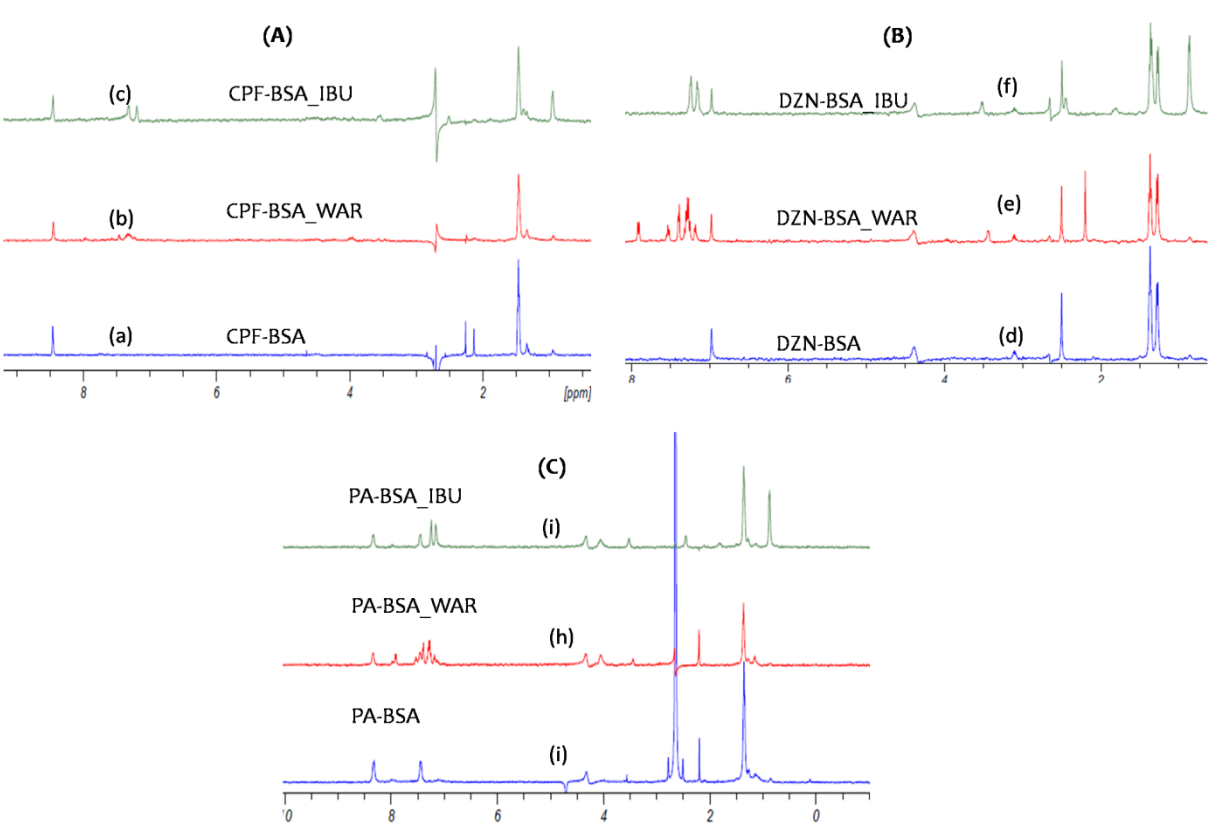

Figure 3.7 : (A) (a) ^{1}H STD NMR of 10 µM BSA, 400 µM CPF without the site probe; (b) ^{1}H STD NMR of 10 µM BSA, 400 µM CPF in the presence of 400 µM WAR; (c) ^{1}H STD NMR of 10 µM BSA, 400 µM CPF in the presence of 400 µM IBU, (B) (a) ^{1}H STD NMR of 10 µM BSA, 400 µM DZN without the site probe; (b) ^{1}H STD NMR of 10 µM BSA, 400 µM DZN in the presence of 400 µM WAR; (c) ^{1}H STD NMR of 10 µM BSA, 400 µM DZN in the presence of 400 µM IBU, (C) (A) (a) ^{1}H STD NMR of 10 µM BSA, 400 µM PA without the site probe; (b) ^{1}H STD NMR of 10 µM BSA, 400 µM PA in the presence of 400 µM WAR; (c) ^{1}H STD NMR of 10 µM BSA, 400 µM PA in the presence of 400 µM IBU. Spectra are taken at 298 K on a 500 MHz spectrometer with a room temperature probe. NS = 2048, TD = 32 K, sat pulse = –0.6 ppm for 2.0 s.

Furthermore, in the presence of WAR, the change is more noticeable. These results revealed that CPF is bound to BSA at site I. The same experiment is followed for PA and DZN which showed that the competition occurred with PA and DZN from both sites I and II of BSA and more remarkable change is observed for site I (Figure 3.7 (B and C)). Thus, PA and DZN preferentially bind to BSA at site I. From the site-marker experiments, it confirmed that the two binding sites are involved in the OP-BSA interaction, but for the above-mentioned OP, the prominent binding site is located in the site I.

3.4.4 Competition STD NMR for Ligands mixture

It is confirmed from site marker experiments that CPF, DZN, and PA access the same site, site I for binding to BSA. Therefore, in a mixture of these OP, they can compete with each other for the same binding site. For this reason, the competition STD NMR spectroscopy is used for competitive binding studies of the ligand mixture. It is given in literature that in a mixture of the competitive ligands, if one ligand exhibits a higher binding affinity towards the particular sites of the given protein than the other ligand, the receptive STD intensity of low-affinity ligand will decrease or vice-versa [Wang et al, 2004]. However, the two ligands exhibit different binding sites to the given protein; there will be no effects on the STD signals obtained for the ligands.

STD NMR for compound mixture analysis for both high and low-affinity ligands is essential for the determination of structure-activity relationship. The combination of routine STD NMR method with competition STD NMR method is used to investigate the mixture of ligands indirectly by considering the STD peak intensities. If the ligands possess the same binding site for the macromolecule under study then the STD peak intensities due to the weak binding ligand will decrease or disappear in comparison to the high-affinity ligand [Angulo et al, 2010; Angulo and Nieto, 2011; Monaco et al, 2017a; Tanoli et al, 2015; Wang et al, 2004]. In the present study, two sets of samples are used to carry out the competition STD experiments: (A) Set I: CPF-DZN; (B) Set II: DZN-PA as illustrated in Figure 3.8 (A) and (B).

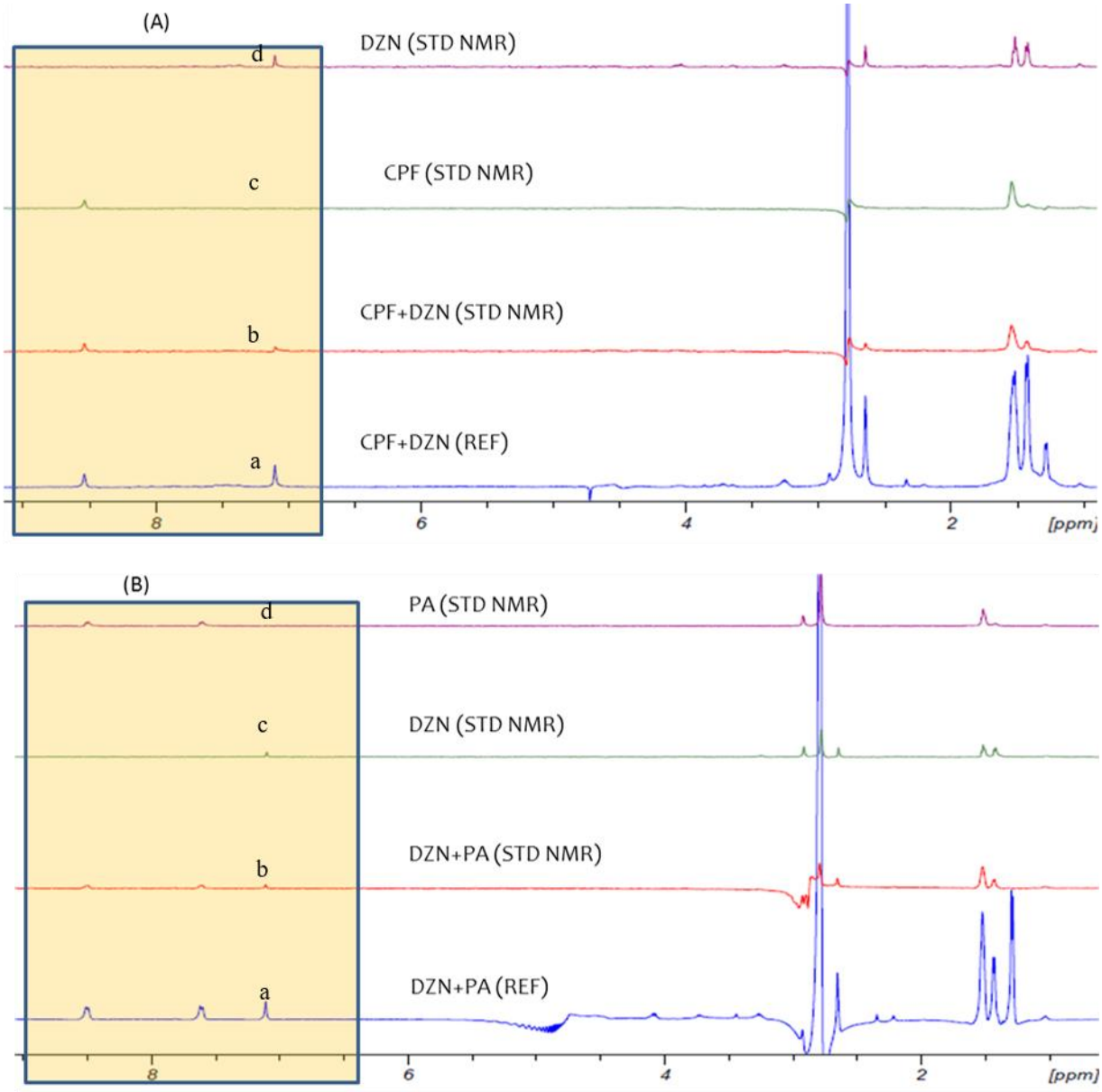

Figure 3.8 : The STD NMR spectra of the (A) CPF-BSA in the presence of DZN, (B) DZN-BSA in the presence of PA. Upon addition of the high-affinity ligand, the STD signals of weak affinity ligand reduced.

It is clear from the Figure 3.8 that for Set I case, the reduction in DZN STD signals occur, which confirms the high affinity of CPF towards BSA. Further, the same set of experiments are performed for Set II samples, and a significant difference in affinity of the two OP (PA binding is stronger than DZN) is clearly observed. Figure 3.9 further exhibits the STD competition binding experiment performed for the Set III sample consisting of a mixture of CPF-PA-DZN. However, due to structural similarity of all the test OP leading to significant peak overlap between CPF and PA in the ring moiety as well as in the phosphate moiety of all the OP, no meaningful conclusion can be drawn.

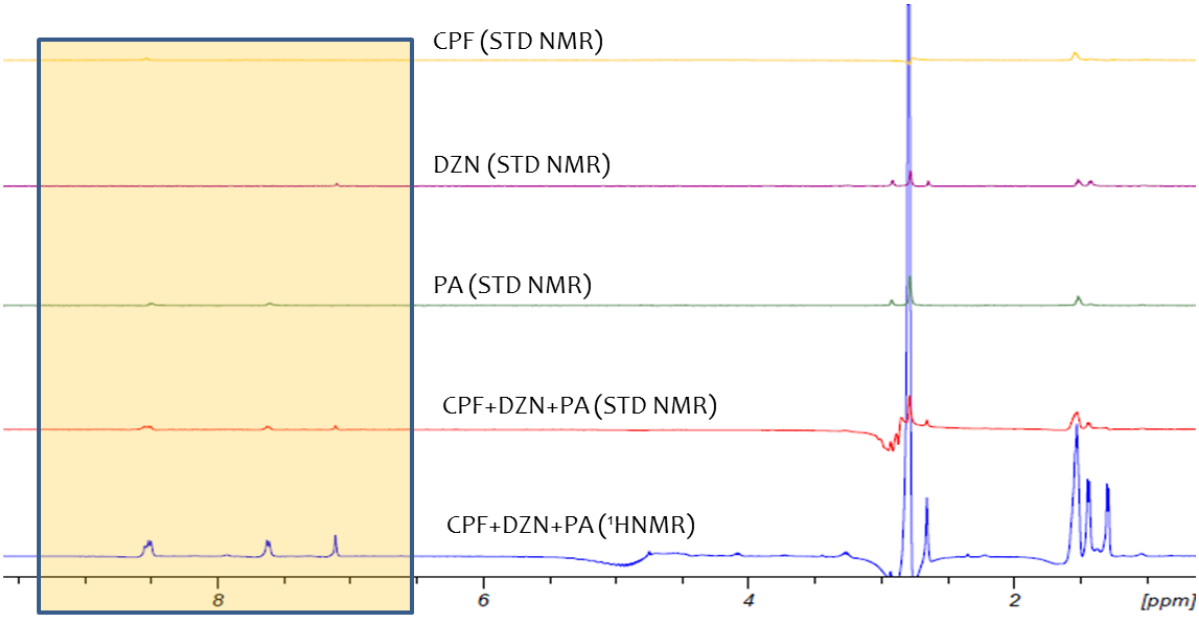

Figure 3.9 : STD-NMR (CPF/DZN/PA with BSA) spectra in a mixture with equal concentration. The STD-NMR spectra are performed with 40 µM BSA with 2 s saturation time at 298 K.

3.5 MOLECULAR DOCKING STUDY

Molecular docking is used as a complementary method to determine the binding sites between ligand-protein. BSA exhibit mainly two binding sites *viz*. site I, and site II and these sites are located in hydrophobic cavities in subdomain IIA and IIIA, respectively. Figure 3.10 represents the conformation between BSA and the test OP.

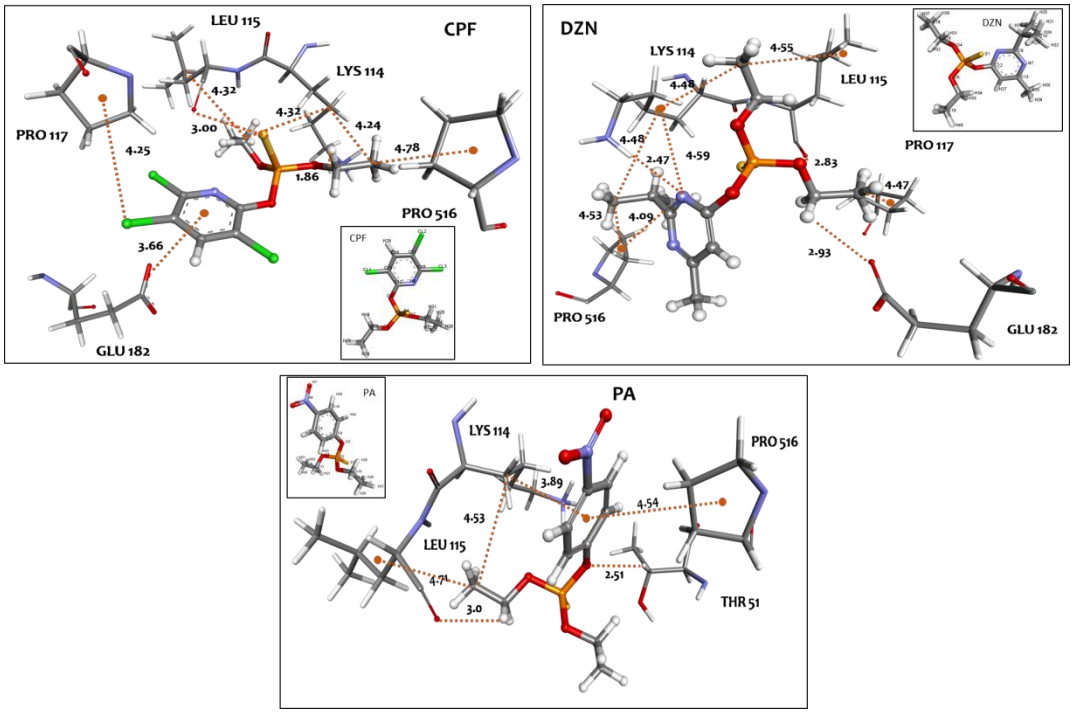

Figure 3.10 : Molecular docking results for CPF, DZN, and PA.

It is evident from Figure 3.10 in CPF–BSA interaction, the CPF molecule is surrounded by some hydrophobic residues with amino acids such as LEU115, LYS114, PRO117, PRO516, and electrostatic interactions with residue GLU 182. While the interaction of DZN-BSA is achieved through LEU115, LYS114, PRO117, PRO516 by hydrophobic forces, whereas in the case of BSA–PA system, the OP is surrounded by THR518, LEU115, PRO516, and LYS114 residues. Moreover, DZN formed three hydrogen bonds with the GLU 118, LEU115 and, LYS114 residues with bond distance 2.93, 2.83, and 2.47 Å, respectively. On the other hand, PA forms two hydrogen bonds with residues LEU115, THR518 with 2.50, and 3 Å bond distance. In contrast, CPF formed two hydrogen bonds with LEU115, LYS114 residues with a bond distance of 3 and 1.85 Å, respectively. The docking results confirmed that for OP-BSA interaction, the hydrophobic forces are major interaction forces with hydrogen bonds, as shown in Table 3.6**.**

Table 3.6 : Summary of interactions between OP-BSA (CPF, DZN, and PA).

CPF		
Interacting Residues	**Bond Length (Å)**	**Interaction Type**
CPF: C13 - B:PRO516	4.78	Hydrophobic
CPF: CL2 - B:PRO117	4.24	Hydrophobic
CPF: E1 - B:GLU182	3.66	Electrostatic
CPF: S4 - B:LEU115:O	3.0	Hydrogen Bond
CPF: H21 - B:LEU115:O	2.49	Hydrogen Bond
CPF :C14 - B:LEU115	4.32	Hydrophobic
CPF : C14 - B:LYS114	4.31	Hydrophobic
CPF : C13 - B:LYS114	4.23	Hydrophobic
CPF : CL3 - B:PRO117	4.22	Hydrophobic
CPF :O6 - B:LYS114:HZ1	1.85	Hydrogen Bond
DZN		
DZN :H33 - B:GLU182:OE1	2.93	Hydrogen bond
DZN:H34 - B:LEU115:O	2.83	Hydrogen bond
DZN :N6 - B:LYS114:HZ1	2.47	Hydrogen bond
DZN:C18 - B:LEU115	4.5	Hydrophobic
DZN:C11 - B:LYS114	4.47	Hydrophobic
DZN:C10 - B:LYS114	4.59	Hydrophobic
DZN:C18 - B:LYS114	4.48	Hydrophobic
DZN:C19 - B:PRO117	4.47	Hydrophobic
DZN:C10 - B:PRO516	4.09	Hydrophobic
PA		
PA:O3B- THR518:HB	2.50	Hydrogen bond
PA:H22 - B:LEU115:O	3.0	Hydrogen bond
PA- B:PRO516	4.54	Hydrophobic
PA:C18 - B:LYS114	4.52	Hydrophobic
PA - B:LYS114	3.89	Hydrophobic
PA:C18 - B:LEU115	4.70	Hydrophobic

3.6 ISOTHERMAL TITRATION CALORIMETRY

In this section, Isothermal Titration Calorimetry (ITC) has been employed as a complementary method to STD NMR besides quantifying the binding affinity and thermodynamic parameters of the OP-BSA complexes. The thermodynamic parameters and energetics associated with ligand binding to biological macromolecules can be easily analyzed by ITC [Olsson et al, 2008]. It provides detailed information regarding the thermodynamic and binding parameters associated with ligand-protein interactions *viz.* entropy change (ΔS°), enthalpy change (ΔH°), and binding constant (K_A) and binding stoichiometry (n) [Yang et al, 2017]. The ITC parameters also offer information about the nature of the reaction *i.e.,* exothermic and endothermic reaction and molecular forces involved in the binding interactions. The advantage of using ITC is that it can directly measure heat evolved during interaction without requiring chemical modification of reactants [Homans, 2007]. Figure 3.11 represents the ITC titration data recorded for OP-BSA complexes at 298 K.

The upper trace of the Figure 3.11 shows the raw ITC profile of OP-BSA binding. A single OP injection into the BSA solution corresponds to each peak in the isotherm. The heat released per injection is plotted as a function of the molar ratio of OP to BSA in the bottom trace, and the fitting is obtained by following the one-site binding model. Further, from this plot, the association constant (*K*), entropy change (Δ*S*), and enthalpy change (Δ*H*) are directly quantified. The results are given in Table 3.7 illustrate that the OP binds to BSA with moderate affinity. This observation is justified by the literature mentioning that for non-covalent interaction between ligand-BSA, the K_A value falls in the range of 10^4–10^6 M^{-1} [Karthikeyan et al, 2015]. Further, the comparison of K_A values confirms that CPF-BSA interaction is relatively stronger than that of PA-BSA and DZN-BSA. The ITC results are in-line with STD-NMR results. Δ*H* and Δ*S* values can be used to determine the molecular forces involved during ligand-protein interaction according to the theory of Ross and Subramanian [Ross & Subramanian, 1981]. The negative Δ*H* and positive Δ*S* values confirm the hydrophobic and electrostatic interaction for the CPF-BSA system, whereas for PA-BSA and DZN-BSA systems, the results confirm that van der Walls and hydrogen bonds play a significant role in binding reactions.

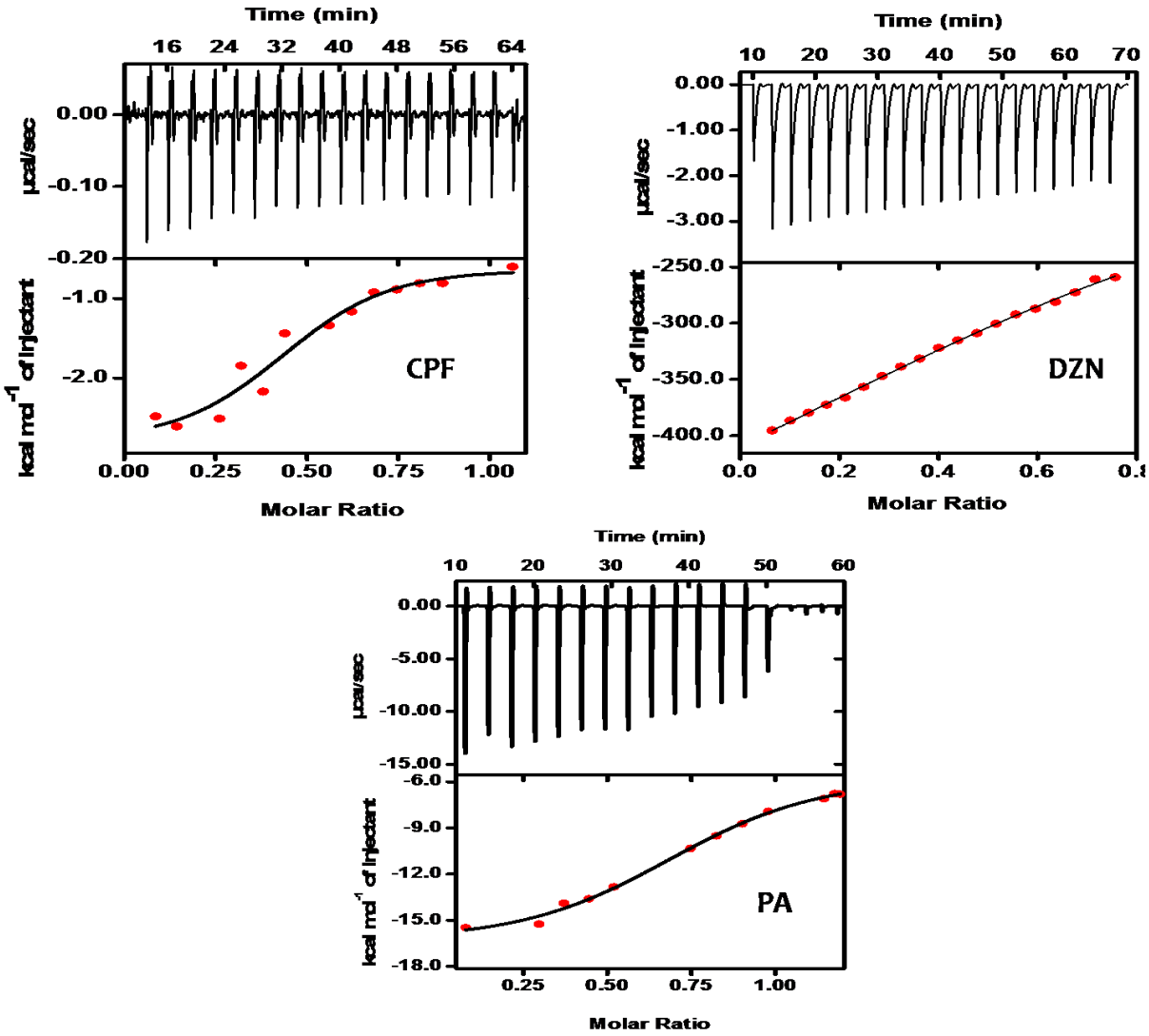

Figure 3.11 : ITC Raw data for the titration of 200 µM OP with 25 µM BSA at pH 7.4.

Table 3.7 : Thermodynamic parameters for interaction of OP with BSA

OP	K_a (M^{-1})	ΔH cal/mol	ΔS cal/mol/K	n
CPF	5.71×10^{5} ±7.84	-6.386×10^{3} ±607.9	4.92	0.45
PA	7.80×10^{4} ±7.84	-1.78×10^{4} ±1.572	-548	1.07
DZN	3.88×10^{4} ±7.84	-7.910×10^{4} ±7.74	-2.63×10^{3}	1.36

3.7 CONCLUSION

To characterize the OP-protein interaction, the STD NMR technique used in the current study proved its advantage over other methods in successfully screening the ligand library. The present study provides a detailed investigation of the interaction of CPF, DZN, and PA with BSA using both experimental (NMR, ITC) and computational approaches (MD). The STD-NMR results, complemented with docking analysis and ITC, reveal that the binding of OP-BSA exhibit a similar binding pattern, in which the ring protons are in close contact with BSA binding site.

The test OP molecules demonstrate the competition binding during interaction with BSA. CPF-BSA shows stronger binding than the other two chosen OP that can be attributed to the fact that CPF molecular structure carries halogen atoms, namely chlorine in the ring moiety that can participate in halogen-bonding with the protein [Lin and Mackerell, 2017; Shinada et al, 2019; Wilcken et al, 2013]. Such halogen bonding increases the binding affinity of a ligand towards a protein. In contrast, both DZN and PA exhibit weaker binding affinity as compared to CPF due to the absence of halogen bonding interaction as well as the probable steric hindrance generated due to the presence of the methylene group on DZN and PA. Site-marker competition STD NMR confirms that the aforementioned OP binds to BSA at the same binding site *i.e.*, site I. Further, competition STD NMR recorded for a mixture of OP with BSA strengthens the above fact by demonstrating the strong binding of CPF over DZN and PA to the same binding site. However, it should be noted here that for the mixture of ligands with overlapped peaks, it is difficult to differentiate the STD effect and further quantification for such regions. Molecular docking results indicate that hydrophobic interaction and hydrogen bonding are the major interacting forces for OP-BSA complexes. ITC results complemented NMR experimental findings as well as molecular docking analysis in terms of binding affinity and the molecular forces, respectively.

In conclusion, the present study enables the characterization of OP-BSA interaction in terms of the strength of the binding that indicates the stability of these complexes. It is clear from these findings that a more stable CPF-BSA complex will allow limited diffusion of CPF within the body while the loosely bound DZN and PA will have a better chance to diffuse to other body tissues [Kragh-Hansen, 2013, Mourik & de Jong, 1978, Silva et al., 2004, Suganthi & Elango, 2017b,Tarhoni et al, 2008]. As per the relevant literature search, this is the first time that an NMR account of OP-BSA interaction has been systematically reported for these three test OP and will be of particular interest in the area of pesticide biosensor designing, ecotoxicology, and environmental risk assessment.

…